

# Quest for a highly connected robust porous metal–organic framework on the basis of a bifunctional linear linker and a rare heptanuclear zinc cluster†

Cite this: *Chem. Commun.*, 2013, **49**, 10516

Received 5th August 2013,  
Accepted 17th September 2013

DOI: 10.1039/c3cc45986a

www.rsc.org/chemcomm

Wen-Yang Gao,<sup>a</sup> Rong Cai,<sup>b</sup> Le Meng,<sup>a</sup> Lukasz Wojtas,<sup>a</sup> Wei Zhou,<sup>cd</sup>  
Taner Yildirim,<sup>ce</sup> Xiaodong Shi<sup>\*b</sup> and Shengqian Ma<sup>\*a</sup>

**A strategy for building highly connected robust MOFs from linear ligands is exemplified by the construction of MTAF-4, a rare (6,9)-connected MOF, based on the custom-designed bifunctional linear ligand, 4-(1,2,3-triazol-4-yl)-benzoate, that connects two types of highly connected zinc cluster moieties generated *in situ*. MTAF-4 is robust and permanently microporous and is capable of adsorbing CO<sub>2</sub>, H<sub>2</sub> and CH<sub>4</sub> under high pressures.**

The past two decades have witnessed the exponential development of metal–organic frameworks (MOFs)<sup>1</sup> as a new type of functional materials. MOFs are built from multidentate organic ligands and metal ions or *in situ* generated metal ion clusters (also known as secondary building units (SBUs)) through coordination bonds. They feature tunable pore sizes, controllable surface areas, and functionalizable pore walls, which can be achieved *via* custom-design of functional organic ligands and judicious selection of SBUs.<sup>2</sup> The designable and modular<sup>3</sup> features of MOFs have offered them great potential for a plethora of applications, such as gas storage,<sup>4</sup> gas separation,<sup>5</sup> catalysis,<sup>6</sup> CO<sub>2</sub> capture,<sup>7</sup> sensors<sup>8</sup> and others.<sup>9</sup> Among various types of MOFs, highly connected structures have been widely pursued given their framework robustness and remarkable surface areas. This is well exemplified by the (3,24)-connected *rht*-topology MOFs<sup>10</sup> which hold the record of experimental Brunauer–Emmett–Teller (BET) surface area<sup>10d</sup>

and the (4,8)-connected *scu*-topology MOFs<sup>11</sup> which exhibit excellent gas adsorption performances. Existing approaches to constructing highly connected MOF structures heavily rely on the utilization of multitopic organic ligands (*e.g.* the *rht*-topology MOFs are mainly based on hexacarboxylate ligands<sup>10</sup> and the *scu*-topology MOFs are built from octacarboxylate ligands<sup>11</sup>), which requires multistep complex organic synthesis. In this contribution, we report an alternative strategy of employing the linear bifunctional ligand with two distinct donor groups that can facilitate the *in situ* generation of multinuclear metal clusters as highly bridged nodes to afford the highly connected robust MOF structure.

As we and others reported previously,<sup>12</sup> the 1,2,3-triazolate donor group featuring three nitrogen atoms as coordination sites favors the formation of highly connected multinuclear metal clusters particularly when in combination with a carboxylate donor group. This makes triazolate–carboxylate bifunctional ligands promising candidates for the construction of highly connected robust MOFs with the *in situ* formed multinuclear metal clusters as highly bridged nodes. Bearing these above in mind, herein, we employed a custom-designed bifunctional linear ditopic ligand, 4-(1,2,3-triazol-4-yl)-benzoate (*tab*), that features both 1,2,3-triazolate and carboxylate donor groups (Fig. 1a), and the self-assembly of the *tab* ligand with Zn(NO<sub>3</sub>)<sub>2</sub> under solvothermal conditions afforded a rare (6,9)-connected robust MOF, termed MTAF-4 (MTAF denotes a metal–triazolate framework), which is based on the *in situ* generated tetranuclear (Fig. 1b) and heptanuclear (Fig. 1c) zinc cluster moieties serving as 6- and 9-connected nodes respectively. MTAF-4 is permanently microporous with a BET surface area of ~1600 m<sup>2</sup> g<sup>-1</sup> and is capable of adsorbing CO<sub>2</sub>, H<sub>2</sub> and CH<sub>4</sub> under high pressures.

The colorless pyramid-shaped crystals of MTAF-4 were harvested by reacting the bifunctional linear ligand, *tab*, with Zn(NO<sub>3</sub>)<sub>2</sub>·6H<sub>2</sub>O in *N,N*-dimethylformamide (DMF) at 135 °C for 3 days. Single-crystal X-ray diffraction analysis† reveals that MTAF-4 crystallizes in the space group *P6<sub>3</sub>/mmc* with a formula [Zn<sub>7</sub>(μ<sub>4</sub>-O)<sub>2</sub>O<sub>3</sub>(*tab*)<sub>9/2</sub>]<sub>2</sub>·[Zn<sub>4</sub>(μ<sub>4</sub>-O)(*tab*)<sub>3</sub>]. It adopts two types of SBUs: one is Zn<sub>4</sub>(μ<sub>4</sub>-O)(CO<sub>2</sub>)<sub>6</sub> (Fig. 1b) and the other is Zn<sub>7</sub>(μ<sub>4</sub>-O)<sub>2</sub>(CO<sub>2</sub>)<sub>3</sub>(C<sub>2</sub>N<sub>3</sub>)<sub>6</sub> (Fig. 1c). The SBU of Zn<sub>4</sub>(μ<sub>4</sub>-O)(CO<sub>2</sub>)<sub>6</sub> is ubiquitous in Zn-based MOFs and serves as a 6-connected node as widely observed in

<sup>a</sup> Department of Chemistry, University of South Florida, 4202 East Flower Avenue, Tampa, Florida, 33620, USA. E-mail: sqma@usf.edu; Fax: +1-813-974-3203; Tel: +1-813-974-5217

<sup>b</sup> Department of Chemistry, West Virginia University, Morgantown, West Virginia, 26506, USA. E-mail: xiaodong.shi@mail.wvu.edu; Fax: +1-304-293-4904; Tel: +1-304-293-4904 ext. 6438

<sup>c</sup> NIST Center for Neutron Research, Gaithersburg, Maryland, 20899, USA

<sup>d</sup> Department of Materials Science and Engineering, University of Maryland, College Park, Maryland, 20742, USA

<sup>e</sup> Department of Materials Science and Engineering, University of Pennsylvania, Philadelphia, Pennsylvania, 19104, USA

† Electronic supplementary information (ESI) available: Details of detailed synthesis of MTAF-4, powder X-ray diffraction patterns, thermogravimetric analysis plots, Ar adsorption isotherm and crystal data for MTAF-4. CCDC 951981. For ESI and crystallographic data in CIF or other electronic format see DOI: 10.1039/c3cc45986a

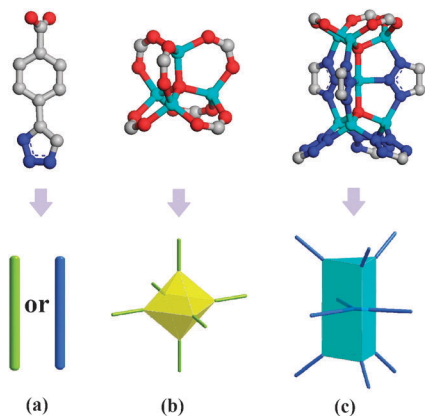


**Fig. 1** Schematic representation of (a) 4-(1,2,3-triazol-4-yl)-benzoate (tab) ligands as linear linkers; (b) tetranuclear zinc clusters as 6-connected nodes; (c) heptanuclear zinc clusters as 9-connected nodes (color scheme: C, gray; O, red; N, blue; Zn, turquoise).

IRMOF series.<sup>13</sup> In comparison, the SBU of  $Zn_7(\mu_4-O)_2(CO_2)_3(C_2N_3)_6$  has not been presented in existing MOFs, and represents a new heptanuclear zinc cluster moiety bridged by carboxylate and 1,2,3-triazolate groups. The new heptanuclear zinc cluster can be considered as two clusters of  $Zn_4(\mu_3-O)(CO_2)_3(C_2N_3)_3$  and  $Zn_4(\mu_3-O)(C_2N_3)_6$  fused through the central five-coordinate Zn atom (Fig. 1c). The central Zn atom connects with two  $\mu_4-O$  atoms along the axial direction and three 2-positioned N atoms of three different 1,2,3-triazole groups of three tab ligands in the equatorial plane; on one side of the equatorial plane, each of the three four-coordinate Zn atoms bonds the  $\mu_4-O$  atom, two O atoms of two different carboxyl groups of two tab ligands, and one 1 (or 3)-positioned N atom of the triazole group of one tab ligand in the equatorial plane of the central Zn atom; on the other side, each of the three four-coordinate Zn atoms connects with the  $\mu_4-O$  atom and three N atoms of three different triazole groups of three tab ligands, with one residing in the equatorial plane of the central Zn atom. Every  $Zn_7(\mu_4-O)_2(CO_2)_3(C_2N_3)_6$  SBU serves as the nine-connected node to link six  $Zn_4(\mu_4-O)(CO_2)_6$  SBUs and three other  $Zn_7(\mu_4-O)_2(CO_2)_3(C_2N_3)_6$  SBUs through nine linear tab linkers, and each  $Zn_4(\mu_4-O)(CO_2)_6$  SBU serves as the six-connected node bridges, six  $Zn_7(\mu_4-O)_2(CO_2)_3(C_2N_3)_6$  SBUs, *via* six tab linkers. This thereby affords an unprecedented (6,9)-connected binodal three-dimensional (3D) net, with the topology of *wyg* (Fig. S1, ESI<sup>†</sup>) whose vertex symbol is  $(3^6 \cdot 4^{18} \cdot 5^9 \cdot 6^3)(3^6 \cdot 4^6 \cdot 5^3)$ . In the overall network of MTAF-4, the ratio of 6-connected tetranuclear and 9-connected heptanuclear zinc clusters is 1:2. There exist regular triangular pores with an edge length of  $\sim 9.9$  Å (atom to atom distance) along the *c* axis (Fig. 2a), and proximately square channels (edge length of  $\sim 11.5$  Å, atom to atom distance), each of which is split by one tab ligand across the diagonal, are observed along the (1,−1,1) direction (Fig. 2b). MTAF-4 is porous and possesses a solvent-accessible volume of 59.5% as calculated using PLATON.<sup>14</sup>

The phase purity of MTAF-4 was verified by powder X-ray diffraction (PXRD) studies, which revealed that the diffraction patterns of the fresh sample are consistent with the calculated ones (Fig. S2, ESI<sup>†</sup>). Thermogravimetric analysis (TGA) of the fresh MTAF-4 sample indicates a weight loss of  $\sim 35\%$  from

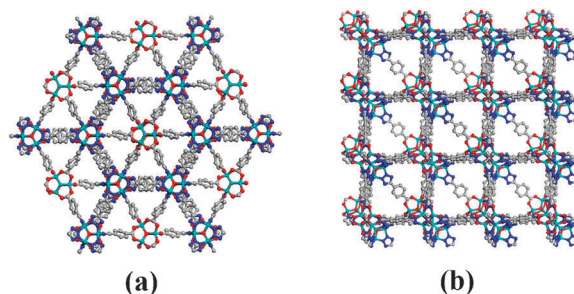


**Fig. 2** (a) Packing picture of MTAF-4 from the *c* direction; (b) packing picture of the MTAF-4 view along the (1,−1,1) direction.

30 to 200 °C corresponding to the loss of guest solvent molecules trapped in the channels. It is followed by a steady plateau from 200 °C to 410 °C before complete decomposition of the framework (Fig. S3, ESI<sup>†</sup>), highlighting the robustness and high thermal stability of this highly connected MOF structure.

To examine the permanent porosity of MTAF-4, gas sorption analysis was performed on the activated sample. As shown in Fig. 3a, the nitrogen adsorption isotherm at 77 K reveals that MTAF-4 exhibits an uptake capacity of  $\sim 420$  cm<sup>3</sup> g<sup>−1</sup> at the saturation pressure with typical type I adsorption behavior, a characteristic of microporous materials. Derived from the N<sub>2</sub> adsorption data, MTAF-4 possesses a BET surface area of 1590 m<sup>2</sup> g<sup>−1</sup> ( $P/P_0 = 0.0001 - 0.1$ ) [corresponding to a Langmuir surface area of 1790 m<sup>2</sup> g<sup>−1</sup> ( $P/P_0 = 0.9$ )], which is slightly lower than the theoretically calculated BET surface area of  $\sim 2000$  m<sup>2</sup> g<sup>−1</sup>. The surface area of MTAF-4 was further confirmed by the Ar adsorption isotherm at 87 K (Fig. S4, ESI<sup>†</sup>), which revealed similar surface area values. Density functional theory (DFT) pore size distribution analysis based on the Ar adsorption data at 87 K indicated that the pore size of MTAF-4 is narrowly distributed at around 12.0 Å (Fig. S5, ESI<sup>†</sup>), which is in good agreement with the channel width observed in crystal structure (Fig. 2b). MTAF-4 can retain its framework integrity after gas adsorption analysis as confirmed by PXRD studies, which further highlights its framework robustness in the absence of guest species (Fig. S2, ESI<sup>†</sup>).

We evaluated the gas storage performances of MTAF-4 under high pressures. As shown in Fig. 3b, MTAF-4 demonstrates a

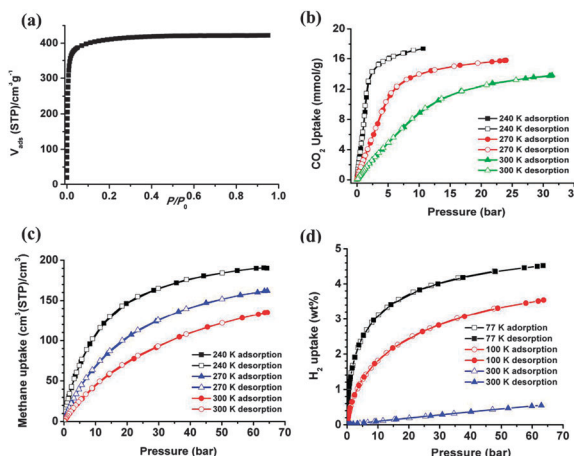


**Fig. 3** (a) N<sub>2</sub> adsorption isotherm of MTAF-4 at 77 K; (b) high pressure CO<sub>2</sub>; (c) CH<sub>4</sub>; and (d) H<sub>2</sub> total sorption isotherms at different temperatures.

total CO<sub>2</sub> adsorption capacity of 17.4 mmol g<sup>-1</sup> at 240 K and 11 bar, 15.8 mmol g<sup>-1</sup> at 270 K and 24 bar, and 13.5 mmol g<sup>-1</sup> at 300 K and 30 bar. The high-pressure CO<sub>2</sub> adsorption capacity of MTAF-4 at room temperature outperforms those of conventional zeolites<sup>15</sup> and activated carbons<sup>16</sup> under the similar conditions; it also surpasses those of some benchmark MOFs, such as 10.2 mmol g<sup>-1</sup> of MOF-505 and 10.7 mmol g<sup>-1</sup> of HKUST-1 at 298 K under a pressure of 35 bar,<sup>17</sup> although MOF-505 and HKUST-1 have larger surface areas than MTAF-4. The higher CO<sub>2</sub> storage capacity of MTAF-4 compared to those of MOF-505 and HKUST-1 could be presumably attributed to the existence of uncoordinated nitrogen atoms of 1,2,3-triazole groups, as exposed nitrogen atoms have been previously demonstrated to serve as Lewis base sites to facilitate CO<sub>2</sub> adsorption in MOFs.<sup>18</sup> Notwithstanding, due to the moderate surface area, the high-pressure CO<sub>2</sub> adsorption performance of MTAF-4 is still moderate compared to some high-surface area porous MOFs.<sup>4,7a,10c,17,19</sup>

The high-pressure CH<sub>4</sub> and H<sub>2</sub> sorption isotherms at a variety of temperatures were also measured. The methane uptake capacity was converted into cm<sup>3</sup>(STP)/cm<sup>3</sup> using the density of MTAF-4 (0.670 g cm<sup>-3</sup>) calculated from the crystallographic data without guest solvent molecules. As shown in Fig. 3c, MTAF-4 can adsorb 190 cm<sup>3</sup>(STP)/cm<sup>3</sup> and 162 cm<sup>3</sup>(STP)/cm<sup>3</sup> at 240 K and 270 K respectively. At 300 K, the total methane uptake capacity of MTAF-4 is 105 cm<sup>3</sup>(STP)/cm<sup>3</sup> at 35 bar and 135 cm<sup>3</sup>(STP)/cm<sup>3</sup> at 64 bar. In terms of high-pressure H<sub>2</sub> adsorption performances, under a pressure of 64 bar, MTAF-4 is capable of adsorbing 4.52 wt% at 77 K, 3.54 wt% at 100 K, and 0.55 wt% at 300 K (Fig. 3d). The high-pressure CH<sub>4</sub> and H<sub>2</sub> adsorption capacities of MTAF-4 are moderate compared to those of some high-surface area MOFs, particularly those with open metal sites.<sup>4,20</sup> This can be presumably ascribed to the moderate surface area of MTAF-4 together with the lack of strong binding sites for CH<sub>4</sub> and H<sub>2</sub> molecules, as evidenced by the relatively low heats of adsorption (Fig. S7 and S8, ESI†).

In conclusion, a rare (6,9)-connected MOF, MTAF-4, was constructed by linking the *in situ* generated six-connected and nine-connected zinc cluster moieties through the bifunctional linear organic ligand of 4-(1,2,3-triazol-4-yl)-benzoate. MTAF-4 demonstrates high thermal stability and framework robustness as well as permanent porosity, which affords it the capability to adsorb CO<sub>2</sub>, H<sub>2</sub> and CH<sub>4</sub> under high pressures. The strategy of employing bifunctional linear ditopic organic ligands to connect highly connected multinuclear metal-containing SBUs generated *in situ* represents a new approach to building highly connected robust porous MOFs. Given the ease of extending and functionalizing the ditopic linear organic ligands, it is anticipated that highly connected robust porous MOFs with higher surface areas and different pore functionalities can be readily achieved for various applications. This line of research is currently underway in our laboratory. Ongoing work in our laboratories also includes the custom-design of new variants of 1,2,3-triazole-based ligands for the construction of functional MTAF materials and exploring them for application in CO<sub>2</sub> capture, sensor and catalysis.

The authors acknowledge the University of South Florida for financial support of this work. X.S. thanks the NSF for financial

support (Grant CHE-0844602). T.Y. acknowledges partial support from the U.S. Department of Energy through BES Grant No. DE-FG02-08ER46522.

## Notes and references

† X-ray crystal data for MTAF-4: C<sub>108</sub>H<sub>60</sub>N<sub>36</sub>O<sub>35</sub>Zn<sub>18</sub>, *f*<sub>w</sub> = 3598.58, hexagonal, *P*<sub>6<sub>3</sub>/mm*c*, *a* = 20.1753(4) Å, *b* = 20.1753(4) Å, *c* = 25.0329(6) Å, *V* = 8824.3(3) Å<sup>3</sup>, *Z* = 1, *T* = 228(2) K, *ρ*<sub>calcd</sub> = 0.677 g cm<sup>-3</sup>, *R*<sub>1</sub> (*I* > 2σ(*I*)) = 0.0615, *wR*<sub>2</sub> (all data) = 0.1947.</sub>

- H.-C. Zhou, J. R. Long and O. M. Yaghi, *Chem. Rev.*, 2012, **112**, 673.
- (a) S. Qiu and G. Zhu, *Coord. Chem. Rev.*, 2009, **253**, 2891; (b) M. O'Keeffe and O. M. Yaghi, *Chem. Rev.*, 2012, **112**, 675.
- O. M. Yaghi, M. O'Keeffe, N. W. Ockwig, H. K. Chae, M. Eddaoudi and J. Kim, *Nature*, 2003, **423**, 705.
- (a) S. Ma and H.-C. Zhou, *Chem. Commun.*, 2010, **46**, 44; (b) M. P. Suh, H. J. Park, T. K. Prasad and D.-W. Lim, *Chem. Rev.*, 2012, **112**, 782.
- J.-R. Li, J. Sculley and H.-C. Zhou, *Chem. Rev.*, 2012, **112**, 869.
- A. Corma, H. Garcia and F. X. Llabres i Xamena, *Chem. Rev.*, 2010, **110**, 4606.
- (a) J. Liu, P. K. Thallapally, B. P. McGrail, D. R. Brown and J. Liu, *J. Chem. Soc. Rev.*, 2012, **41**, 2308; (b) J.-R. Li, Y. Ma, M. C. McCarthy, J. Sculley, J. Yu, H.-K. Jeong, P. B. Balbuena and H.-C. Zhou, *Coord. Chem. Rev.*, 2011, **255**, 1791; (c) K. Sumida, D. L. Rogow, J. A. Mason, T. M. McDonald, E. D. Bloch, Z. R. Herm, T.-H. Bae and J. R. Long, *Chem. Rev.*, 2012, **112**, 724; (d) P. Nugent, Y. Belmabkhout, S. D. Burd, A. J. Cairns, R. Luebke, K. Forrest, T. Pham, S. Ma, B. Space, L. Wojtas, M. Eddaoudi and M. J. Zaworotko, *Nature*, 2013, **495**, 80.
- (a) L. E. Kreno, K. Leong, O. K. Farha, M. Allendorf, R. P. V. Duyne and J. T. Hupp, *Chem. Rev.*, 2012, **112**, 1105; (b) Y. Cui, Y. Yue, G. Qian and B. Chen, *Chem. Rev.*, 2012, **112**, 1126.
- (a) C. Wang, T. Zhang and W. Lin, *Chem. Rev.*, 2012, **112**, 1084; (b) P. Horcajada, R. Gref, T. Baati, P. K. Allan, G. Maurin, P. Couvreur, G. Férey, R. E. Morris and C. Serre, *Chem. Rev.*, 2012, **112**, 1232.
- (a) D. Yuan, D. Zhao, D. Sun and H.-C. Zhou, *Angew. Chem., Int. Ed.*, 2010, **49**, 5357; (b) O. K. Farha, A. O. Yazaydin, I. Eryazici, C. D. Malliakas, B. G. Hauser, M. G. Kanatzidis, S. T. Nguyen, R. Q. Snurr and J. T. Hupp, *Nat. Chem.*, 2010, **2**, 944; (c) B. Zheng, J. Bai, J. Duan, L. Wojtas and M. J. Zaworotko, *J. Am. Chem. Soc.*, 2011, **133**, 748; (d) O. K. Farha, I. Eryazici, N. C. Jeong, B. G. Hauser, C. E. Wilmer, A. A. Sarjeant, R. Q. Snurr, S. T. Nguyen, A. O. Yazaydin and J. T. Hupp, *J. Am. Chem. Soc.*, 2012, **134**, 15016.
- (a) L. Ma, D. J. Mihalczik and W. Lin, *J. Am. Chem. Soc.*, 2009, **131**, 4610; (b) C. Tan, S. Yang, N. R. Champness, X. Lin, A. J. Blake, W. Lewis and M. Schroder, *Chem. Commun.*, 2011, **47**, 4487; (c) W. Zhuang, D. Yuan, D. Liu, C. Zhong, J.-R. Li and H.-C. Zhou, *Chem. Mater.*, 2012, **24**, 18; (d) W. Lu, D. Yuan, T. A. Makal, J.-R. Li and H.-C. Zhou, *Angew. Chem., Int. Ed.*, 2012, **51**, 1580.
- (a) A. Demessence, D. M. D'Alessandro, M. L. Foo and J. R. Long, *J. Am. Chem. Soc.*, 2009, **131**, 8784; (b) W.-Y. Gao, W. Yan, R. Cai, L. Meng, A. Salas, X.-S. Wang, L. Wojtas, X. Shi and S. Ma, *Inorg. Chem.*, 2012, **51**, 4423; (c) J.-P. Zhang, Y.-B. Zhang, J.-B. Lin and X.-M. Chen, *Chem. Rev.*, 2012, **112**, 1001.
- M. Eddaoudi, J. Kim, N. Rosi, D. Vodak, J. Wachter, M. O'Keeffe and O. M. Yaghi, *Science*, 2002, **295**, 469.
- A. L. Spek, *J. Appl. Crystallogr.*, 2003, **36**, 7.
- J. A. Dunne, R. Mariwala, M. Rao, S. Sircar, R. J. Gorte and A. L. Myers, *Langmuir*, 1996, **12**, 5888.
- S. Himeno, T. Komatsu and S. Fujita, *J. Chem. Eng. Data*, 2005, **50**, 369.
- A. R. Millward and O. M. Yaghi, *J. Am. Chem. Soc.*, 2005, **127**, 17998.
- (a) J. An, S. J. Geib and N. L. Rosi, *J. Am. Chem. Soc.*, 2010, **132**, 38; (b) T. Panda, P. Pachfule, Y. Chen, J. Jiang and R. Banerjee, *Chem. Commun.*, 2011, **47**, 2011; (c) W.-Y. Gao, W. Yan, R. Cai, K. Williams, A. Salas, L. Wojtas, X. Shi and S. Ma, *Chem. Commun.*, 2012, **48**, 8898.
- H. Furukawa, N. Ko, Y. B. Go, N. Aratani, S. B. Choi, E. Choi, A. O. Yazaydin, R. Q. Snurr, M. O'Keeffe, J. Kim and O. M. Yaghi, *Science*, 2010, **329**, 424.
- (a) S. Ma, D. Sun, J. M. Simmons, C. D. Collier, D. Yuan and H.-C. Zhou, *J. Am. Chem. Soc.*, 2008, **130**, 1012; (b) T. A. Makal, J.-R. Li, W. Lu and H.-C. Zhou, *Chem. Soc. Rev.*, 2012, **41**, 7761.